
1 **Supplemental data**

2

3 The following supplemental data are available

4 **Supplemental Figure S1.** Identification of *cr-osatp4* and *rps8* editing defects in *cr-osatp4*

5 **Supplemental Figure S2.** Subcellular localization of OsATP4-YFP when transiently
6 expressed in rice protoplasts

7 **Supplemental Figure S3.** RNA editing of *rps8-182* in *ppr676-1*

8 **Supplemental Figure S4.** *rps8* editing defects in the W104 and C015 rice accessions

9 **Supplemental Figure S5.** RNA gel blot hybridization of *rpl16* transcripts in C015

10 **Supplemental Figure S6.** Accumulation of rRNAs in WT and *osatp4*

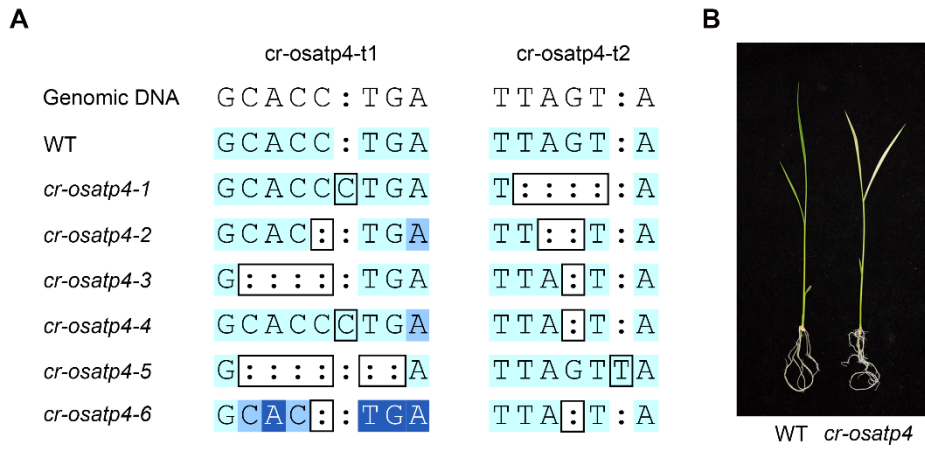
11 **Supplemental Table S1.** The editing efficiency of WT and *osatp4* under both 30°C and 20°C
12 conditions

13 **Supplemental Table S2.** List of oligonucleotides used in this study

14

15 **Supplemental Figure S1.**

16



17

18 **Supplemental Figure S1. Identification of *cr-osatp4* mutants**

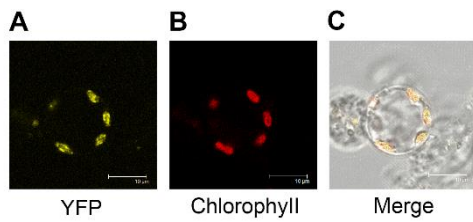
19 **(A)** CRISPR/CAS9 mutant lines of *OsATP4* (abbreviated as *cr-osatp4-1*, *cr-osatp4-2*,
 20 *cr-osatp4-3*, *cr-osatp4-4*, *cr-osatp4-5*, and *cr-osatp4-6*, respectively). The mutant lines were
 21 verified by PCR-based sequencing. Sequenced PCR product of the sgRNA target regions
 22 (*cr-osatp4-t1* and *cr-osatp4-t2*) of WT and the CRISPR/CAS9 mutants were aligned with the
 23 genomic DNA sequence by Sequencher software. The missing/inserted base(s) are marked
 24 with black box. The background blue shading of bases indicates confidence levels of the
 25 nucleotide identity at that position: the darkest blue shading indicates low confidence and the
 26 lightest blue indicates high confidence. **(B)** The phenotype of *cr-osatp4* mutant at 20 °C.

27

28

29 **Supplemental Figure S2.**

30

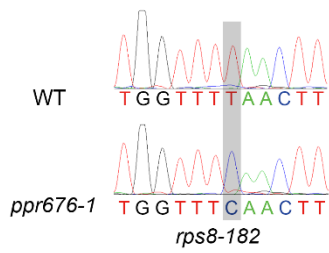


32 **Supplemental Figure S2.** Subcellular localization of OsATP4-YFP when transiently
33 expressed in rice protoplasts

34 (A) Yellow fluorescence signals of P35S:OsATP4:YFP. (B) Chlorophyll autofluorescence
35 signals. (C) Merged images of (A) and (B).

36

37 **Supplemental Figure S3.**



38

39 **Supplemental Figure S3.** RNA editing of *rps8-182* in *ppr676-1*

40

41 Sequence chromatograms of nucleotide sequences including the RNA editing site of
42 *rps8-182* in *ppr676-1*, which was generated by CRISPR/Cas9 system in a Nipponbare
43 background.

44

45

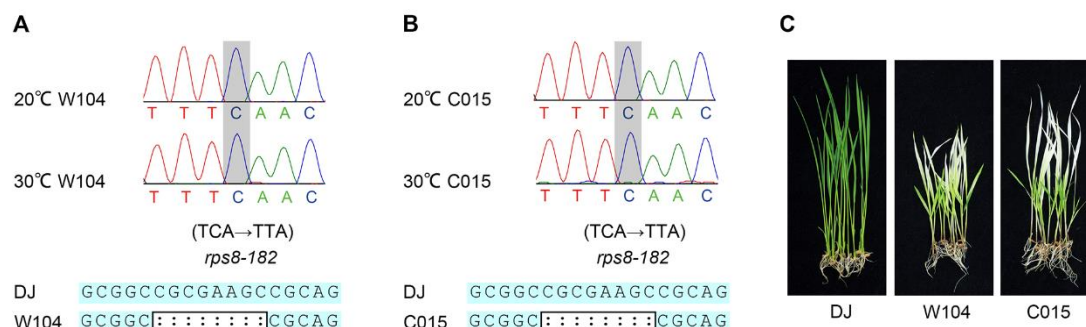
46

47

48

49 **Supplemental Figure S4.**

50



51

52

53 **Supplemental Figure S4. *rps8* editing defects in the W104 and C015 rice accessions**

54 The sequence chromatograms of nucleotide sequences including the RNA editing sites

55 of *rps8-182* in W104 (**A**) and C015 (**B**) at 30 °C and 20 °C. The editing site of *rps8-182*

56 is shaded in gray. *rps8-182* was unedited in W104 and C015 under both conditions.

57 The *DUAL1* gene in W104 and C015 were aligned with genomic DNA sequence of DJ

58 (Dongjin) by Sequencher software. The 8 bp deletion base(s) in W104 and C015 are

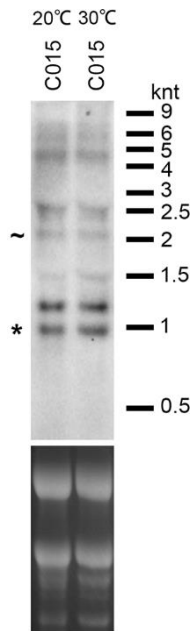
59 marked with black box. (**C**) Phenotypes of Dongjin (DJ), W104 and C015 at 20 °C.

60

61

62 **Supplemental Figure S5.**

63



64

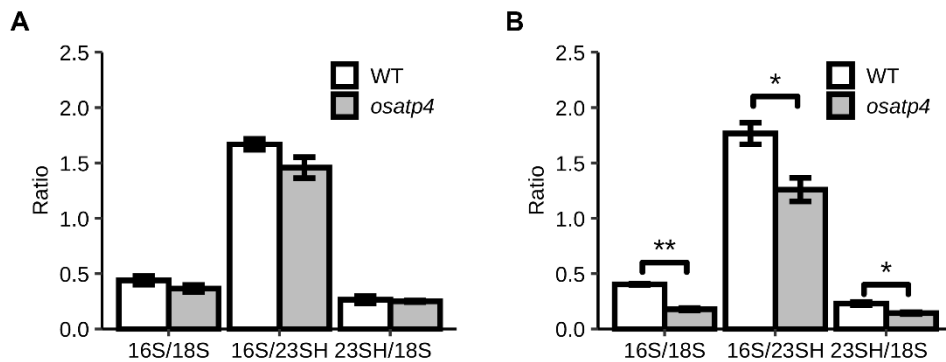
65

66 **Supplemental Figure S5. RNA gel blot hybridization of *rpl16* transcripts in C015**

67 Total leaf RNA (20 µg/lane) of C015 was analyzed by RNA gel blot using a *rpl16*
68 exon 2 probe shown in Fig 6. The positions of RNA size markers are shown on the
69 right side. ~ and * indicate the unspliced and spliced forms of processed *rpl16-rpl14*
70 transcripts, respectively, according to previous results of maize *atp4* (Zoschke et al.,
71 2013b). The ethidium bromide stained gels are shown below to indicate equal sample
72 loading.

73

74 **Supplemental Figure S6.**



75

76 **Supplemental Figure S6.** Accumulation of rRNAs in WT and *osatp4*

77 The ratios of plastid 16S rRNA (component of the 30S subunit) to cytosolic 18S,
78 plastid 16S rRNA to plastid 23SH rRNA (component of the 50S subunit), and plastid
79 23SH rRNAs to cytosolic 18S rRNA are shown for the WT and *osatp4*. “23SH” is a
80 1.1 kb fragment of the 23S rRNA (post-transcriptionally cleaved) in the 50S subunit
81 of the chloroplast ribosome (“hidden break” product of the 23S rRNA) (Tiller et al.
82 2012). Data were obtained from three biological replicates for each plant line, and
83 error bars indicate SE. Significant differences are marked with asterisks according to
84 t-test (**: $P < 0.01$; *: represent $P < 0.05$).

85 **(A)** rRNA ratio in the WT and *osatp4* grown at 30 °C.

86 **(B)** rRNA ratio in the WT and *osatp4* grown at 20 °C.

87

88

89

90 **Supplemental Table S1.**

91 **Supplemental Table S1.** The editing efficiency of WT and *osatp4* under both 30°C and 20°C

92 conditions

93

editing site	30°C condition		20°C treatment	
	WT	<i>osatp4</i>	WT	<i>osatp4</i>
<i>atpA-1148</i>	0.92	0.93	0.95	0.94
<i>ndhA-473</i>	0.94	0.96	0.99	0.95
<i>ndhA-563</i>	0.99	0.98	0.99	0.99
<i>ndhA-1070</i>	0.55	0.54	0.88	0.85
<i>ndhB-467</i>	0.99	0.99	0.99	0.99
<i>ndhB-586</i>	0.80	0.80	0.85	0.85
<i>ndhB-611</i>	0.80	0.80	0.90	0.90
<i>ndhB-704</i>	0.93	0.91	0.90	0.93
<i>ndhB-737</i>	0.50	0.50	0.70	0.70
<i>ndhB-830</i>	0.10	0.10	0.10	0.10
<i>ndhB-836</i>	0.89	0.90	0.90	0.90
<i>ndhB-1481</i>	0.71	0.78	0.77	0.83
<i>ndhD-878</i>	0.95	0.96	0.98	0.99
<i>ndhF-62</i>	0.63	0.71	0.80	0.86
<i>ndhG-5-UTR-10</i>	0.54	0.61	0.88	0.90
<i>rpl2-2</i>	0.59	0.61	0.66	0.66
<i>Rps14-80</i>	0.70	0.70	0.90	0.90
<i>rpoB-467</i>	0.16	0.23	0.47	0.43
<i>rpoB-545</i>	0.40	0.40	0.48	0.55
<i>rpoB-560</i>	0.60	0.60	0.80	0.80
<i>rpoC2-4106</i>	0.77	0.77	0.79	0.81
<i>rps8-182</i>	0.87	0.08	0.98	0.06
<i>ycf3-185</i>	0.84	0.84	0.86	0.82

94

95

96 **Table S2** List of oligonucleotides used in this study

Primer name	primers	Application
P1	AGCCAAACCTGGTCGTGTAC	Genotyping
P2	TTGAGATGCGACTCGAACAC	
P3	CCACAGTTTTTCGCGATCCAGACTG	
q-F	GGGCATCCTGAACGAGAT	qRT-PCR of OsATP4
q-R	TAGCAACGGATGAGCGAG	
Pcom-F	GGGGTACCCACTGGCCAAGTTACCAATTT	Complementation of <i>osatp4</i>
Pcom-R	GGGGTACCGGGGTATGCTTGGACTGAAA	
PsmrT1-U3-F	GGCAGCAGTGGTCGCTGCACCTGA	CRISPR-Cas9 constructs
PsmrT1-U3-R	AAACTCAGGTGCAGCGACCACTGC	
PsmrT2-U6a-F	GCCGAAATCGGCAGAGTTAGTAG	
PsmrT2-U6a-R	AAACCTACTAACTCTGCCGATTT	
Hpt-F	AGAATCTCGTGCTTTCAGCTTCGA	Southern blot analysis
Hpt-R	TCAAGACCAATGCGGAGCATATAC	
Adapter attB1	GGGGACAAGTTTGTACAAAAAAGCAGGC T	Subcellular localization analysis
Adapter attB2	GGGGACCACTTTGTACAAGAAAGCTGGGT	
PtargetATP4-F	AAAAAGCAGGCTTCACCATGGCTTCCCCTT CCTCCCT	
PtargetATP4-R	AGAAAGCTGGGTGCACCGCTACTAACTCTG CCGA	
editing-ndhB-1F	GGAAATAGCATGGAATAAGGTTTG	RNA editing analysis
editing-ndhB-1R	TTCCTGGGGAGTTATACATTTGTG	
editing-ndhB-2F	ATTTACTCATGGGTGGGGCA	
editing-ndhB-a	TCCTTCGTAGACGTCAGGAG	

editing-ndhB-b	CCCACTCCAGTCGTTGCTTT
editing-ndhB-2R	ATTACCCTAGCGCCCATTC
editing-rpoB-F	GGATGCTGTGTATGAATCAC
editing-rpoB-R	CTTGGCTTGTGTATCCGTC
editing-rps8-F	ACCTCTATAAGAAACGCGGACA
editing-rps8-R	AGACTTCTCCCCAATTCTGTT
editing-rps14-F	CCATCTAGGATTAGAACCGT
editing-rps14-R	ATCTTGTTGCACCCGGTAAC
AtpA-1148-F	ACGTTGGATGGGGTATTTCCGTTTCCAGAG
AtpA-1148-R	ACGTTGGATGCCGCGAATTGAGCTAATTCC
AtpA-1148-E	AAACAAGTAGCTGGCAAAT
ndhA-473-F	ACGTTGGATGATAGATTGAGCGGCAGCTCG
ndhA-473-R	ACGTTGGATGATTGGTCTTCTTATGGCAGG
ndhA-473-E	GCTCGTAGACCACCT
ndhA-563-F	ACGTTGGATGGCTGCCGCTCAATCTATTAG
ndhA-563-R	ACGTTGGATGGACTGTGCTTCAACTATATC
ndhA-563-E	CTATCTCTACTATCCAACAGTT
ndhA-1070-F	ACGTTGGATGCTATTTCCCTGGGCAATCTC
ndhA-1070-R	ACGTTGGATGTTGAGAGGACTTTTGTGTTG
ndhA-1070-E	GCAATCTCTTATTAACAACCTTCTT
ndhB-704-F	ACGTTGGATGCCCCAGGAATTTCAATTGCG
ndhB-704-R	ACGTTGGATGTAGACGTCAGGAGTCCATTG
ndhB-704-E	GAATTTCAATTGCGCTTATAT

ndhB-836-F	ACGTTGGATGGATGCCATTCGTTTGATGAG
ndhB-836-R	ACGTTGGATGCACTCCAGTCGTTGCTTTTC
ndhB-836-E	AGAATTCGCGTGGCT
ndhB-1481-F	ACGTTGGATGGACTGTATGTGTGATAGCAT C
ndhB-1481-R	ACGTTGGATGTAAAAGAGGGTATCCTGAGC
ndhB-1481-E	CGTATGTGTGATAGCATCTACTATAC
ndhD-878-F	ACGTTGGATGGGAATTGTTACCTCATGCTC
ndhD-878-R	ACGTTGGATGTTGAAATTGCGTTGGCCAAG
ndhD-878-E	GATGCAAATAATCTATGCAGCTT
ndhF-62-F	ACGTTGGATGAATCCCTCTTCTCCCACTTC
ndhF-62-R	ACGTTGGATGAAAGCCCATATGCGACGAAG
ndhF-62-E	CCCACTCCAGTTATTATGT
ndhG-5-UTR-10-F	ACGTTGGATGGTATTGGCCCAGGTAAATCC
ndhG-5-UTR-10-R	ACGTTGGATGCCTAATCCCTTTTTTCTTCC
ndhG-5-UTR-10-E	CCAGGTAAATCCATTATGGATAA
rpl2-2-F	ACGTTGGATGTGCTCGGGATAGGTGTTTTG
rpl2-2-R	ACGTTGGATGACCCTTCAACCGGGTTATTC
rpl2-2-E	CTTCGTTTTGTATAAATGTTTCGCC
rpoB-467-F	ACGTTGGATGCACCGGGACTATAATATCAG
rpoB-467-R	ACGTTGGATGACGCGAGCCCATATCCTTTC
rpoB-467-E	TAAGATTGGGGAGGAAGAT
rpoB-545-F	ACGTTGGATGGGCTCGCGTGAGTAGAAAAC
rpoB-545-R	ACGTTGGATGTCAGGGTAGGAAACATTATC

rpoB-545-E	ACAAAAGATATCTATTCTAGTTCTAT	
rpoC2-4106-F	ACGTTGGATGGGGTTTCCGAAGATGGAATG	
rpoC2-4106-R	ACGTTGGATGATCGATTCATCCAAAGCCCG	
rpoC2-4106-E	AAGATGGAATGTCTAATGTTTTTT	
rps8-182-F	ACGTTGGATGGTTCGGAAACATCAGGAAAG	
rps8-182-R	ACGTTGGATGTTCCCTTTCTAGTCTTTCTC	
rps8-182-E	ATGAAAGTAACAGATATTTCTTGGTTT	
ycf3-185-F	ACGTTGGATGCGATCATAGGGATCACTTTC	
ycf3-185-R	ACGTTGGATGATGTTGGCTCAATCCGAAGG	
ycf3-185-E	ATATGGATCACTTTCTAGTCGC	
Nor-rps8-F	ATGGGCAAGGACACTATTGC	Northern blot analysis
Nor-rps8-R	TTACCATATATAACATAAGACTTCTCCCC	
Nor-rpl16-F	CCAAAAGAACCAGATTTTCGTAAACA	
Nor-rpl16-R	ACCGAAGAAATTGACTTCGTATGG	

97

98